Elastic Behavior of Woven Fabric Composites: I—Lamina Analysis

N. K. NAIK AND P. S. SHEMBEKAR
Aerospace Engineering Department
Indian Institute of Technology
Powai, Bombay 400076
India

(Received March 22, 1991)
(Revised August 22, 1991)

ABSTRACT: Two-dimensional models are presented for the elastic analysis of a plain weave fabric lamina. These models take into account the actual fabric structure by considering the fiber undulation and continuity along both the warp and weft directions, possible presence of gap between adjacent yarns, actual cross-sectional geometry of the yarn and possible unbalanced nature of the plain weave fabric. Typical studies on the effect of fiber undulation and lamina thickness on the in-plane elastic constants are presented. A large discrepancy, similar to that reported in literature, is found between the predicted elastic moduli of plain weave fabric lamina by 1D WF models and experimental results. On the other hand, the predictions of 2D WF models are fairly good since the two-dimensional extent of the fabric is considered in these models.

KEY WORDS: woven fabric lamina, plain weave, undulation, elastic constants, 2D WF models, gap between adjacent yarns.

INTRODUCTION

A REVIVAL OF interest in the textile composites is observed in recent years. Although textile composites have long been recognized for their applications in the primary and secondary load bearing structures, understanding of the elastic and strength behavior of textile composites is still in its infancy. Woven fabric (WF) composites represent a class of textile composites in which two or more yarn systems are interlaced at an angle. WF composites provide more balanced properties in the fabric plane and higher impact resistance than unidirectional (UD) composites. The interlacing of yarns provides higher out-of-plane strength which can take up the secondary loads due to load path eccentricities, local buckling etc. As the handling of woven fabrics is easier, fabrication of WF composites becomes less laborious. The manufacturing errors are also reduced. These advantages are obtained at the cost of in-plane stiffness and strength properties due to the undulation of yarns.

0021-9983/92/15 2196-30 $6.00/0

The elastic and strength behavior of WF composites depends on the fabric structure. A number of parameters are involved in determining the fabric structure such as the weave, density of yarns in the fabric, fabric count, characteristics of warp and fill yarns, characteristics of fibers and factors introduced during weaving such as yarn crimp etc. Analytical models are therefore necessary to study the effects of various parameters on the behavior of woven fabric composites and to select an efficient fabric structure for a specific application.

Three different types of models are available in literature: elementary, laminate theory and numerical models [1]. The elementary and laminate theory models deal with WF lamina whereas the numerical models have been used for both WF lamina and laminate analysis.

The elementary models tried to give simple estimates of elastic properties of WF lamina. WF lamina was modeled as a laminate of UD laminae, as a network of straight fiber bundles within a prism of matrix material, as a series of curved beams on elastic foundations and as a homogeneous anisotropic material. Closed form solutions have been used considering the fiber curvature [1].

Halpin et al. [2] used laminate analogy for predicting the elastic stiffnesses of 2- and 3-dimensional composites. The warp and fill yarns in the unit cell of a WF lamina were modeled as angle-ply laminates which were then stacked to form balanced and symmetrical laminates. The theoretical results for WF lamina were shown to be only qualitatively correct.

Ishikawa and Chou [3–6] have presented three models to analyze WF composites. These are the mosaic model, fiber undulation model (crimp model) and bridging model. These models are called laminate theory models since the basic assumption involved is that the classical lamination theory (CLT) is valid for every infinitesimal piece of a repeating region of the WF lamina.

In the mosaic model, fabric was idealized by omitting the fiber continuity and undulation. Thus the WF lamina was regarded as an assemblage of pieces of asymmetrical cross-ply laminates. The two-dimensional extent of the lamina was simplified to two one-dimensional models viz. parallel model and series model depending on the arrangement of cross-ply laminates in the lamina. The parallel or iso-strain model was based on the assumption of constant strain state in the WF lamina mid-plane. In the series or iso-stress model, the assumption of constant stress was made. The disturbance of stress and strain near the interface of the interlaced region was neglected. The parallel model gave upper bounds and the series model gave lower bounds of in-plane stiffness constants. The continuity and undulation of fibers in a fabric were considered in the fiber undulation model. This model is an extension of the series model. It was assumed that the configuration normal to the loading direction does not vary. The fiber undulation model was suitable only for weaves with a lower number of repeats, such as plain weave. The in-plane stiffness constants obtained by the fiber undulation model were lower than those obtained by the mosaic series model. Both the mosaic and fiber undulation models considered a one-dimensional strip of a fabric; therefore, these models are not accurate. The bridging model was developed to analyze the WF lamina with satin weave fabric. The undulation and continuity of yarns were considered only along the loading direction. This model was a combination of

series model and parallel model. A good agreement between experimental values and bridging model predictions was obtained. Reference [7] deals with a closed form solution for plain weave WF lamina elastic constants. A WF lamina was modeled as an assemblage of UD warp and fill yarns and a resin layer. Considering the yarn undulation, equivalent UD lamina properties were determined. Then using CLT, the elastic constants of the WF lamina were found out. In this analysis, undulation of the yarn normal to loading direction was not considered.

The numerical models involved the use of the finite element method to analyze the elastic behavior of WF composites. Ishikawa and Chou applied the finite element method to the two- and three-dimensional mosaic model as well as the fiber undulation model [3]. Raju et al. [1] used three-dimensional finite element analysis for the three-dimensional mosaic model. A superposition method was used in this analysis. Using three-dimensional finite element anlaysis, Whitcomb [8] analyzed plain weave composites. He studied the effect of tow wavinesses on the effective moduli, Poisson's ratio and internal strain distributions. He found that the in-plane moduli decreased almost linearly with increasing tow waviness. Also, it was found to cause large normal and shear strain concentrations in the composites subjected to uniaxial load.

Based on photomicrographic study, Dow et al. [9] developed models for various woven fabric composites. The analytical predictions of the elastic properties based on finite element analysis were found to be in good agreement with experiments for satin weaves in tension but less for plain weaves and in compression.

Zhang and Harding [10] have used the strain energy equivalence principle with the aid of the finite element method for the micromechanics analysis of the elastic constants of a plain weave fabric lamina. The plain weave fabric lamina was modeled by assuming the undulation in one direction only. It was suggested that the method should be extended to the case of a two-dimensional undulation model.

The elementary and laminate theory models, although simple, neglect the two-dimensional extent of the fabric. These models consider balanced closed weaves only, whereas in practice the fabric can have unbalanced open weave. The numerical models, on the other hand, can be used for general weave geometry and can give internal stress, strain distribution, but lack simplicity.

The objective of the current paper is to develop a simple, yet generalized, model which considers the two-dimensional extent of the fabric, and to study the effect of various parameters of fabric geometry. Such a model would be useful for the prediction of in-plane elastic constants and selection of fabric geometry for a particular application. The present study is confined to plain weave fabric lamina.

WOVEN FABRIC STRUCTURE

An orthogonal 2D woven fabric consists of two sets of interlaced yarns (Figure 1). The lengthwise set is called warp and the crosswise set is called fill (weft). Any weave repeats on a certain number of warp and fill yarns. The repeat is a complete representative unit cell of the weave. Various types of weaves can be

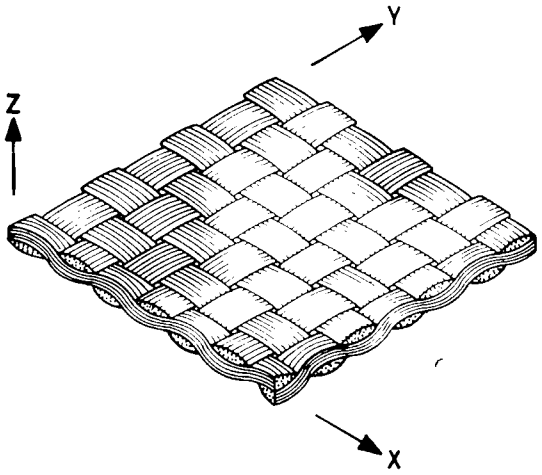

Figure 1. *Plain weave fabric structure.*

identified by the repeating patterns in both directions, defined by geometrical quantities n_x^f and n_x^w. The number n_x^f indicates that a warp yarn is interlaced with every n_x^f-th fill yarn and n_x^w means that a fill yarn is interlaced with every n_x^w-th warp yarn. Based on the repeat, the weaves are classified as plain, twill, satin etc. A woven fabric can be balanced or unbalanced depending on the number of counts, fineness and crimp of the warp and fill yarns. Linear density is the weight of the yarn per unit length which is a measure of fineness of the yarn and is given by tex number (gm/Km). The fabric count is the number of yarns per unit length along the warp or fill direction. Based on the fabric count and width of the yarn, the gap between adjacent yarns can be found. The woven fabric nomenclature used here is presented in Figure 2. Crimp is another parameter which affects the fabric properties. The warp or fill crimp is calculated by expressing the difference between the straightened yarn length and fabric sample length, as a percentage of fabric sample length [11]. A fabric with different crimps in the warp and fill directions can be made (Figure 3). The increase of crimp in one direction of the fabric reduces it in another direction. The thickness of the fabric is closely related to the ratio of crimps. The weaving pattern shown in Figure 3(c) is considered in the present analysis. The term "yarn" is used here to represent individual filaments, untwisted fiber bundles, twisted fiber bundles or rovings.

WOVEN FABRIC COMPOSITE MODELS

The two-dimensional woven fabric models presented here are essentially the extension of 1D models [6]. The 1D models analyze a one-dimensional strip which does not completely represent the actual fabric structure. The two-dimensional representation of the fabric considered in the present analysis takes

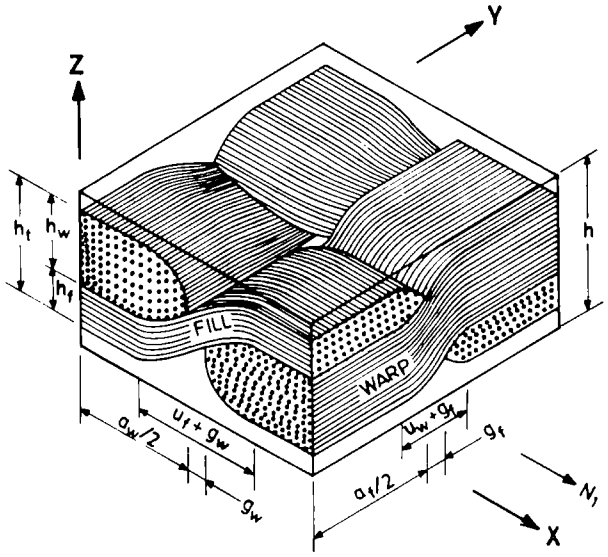

Figure 2. *Woven fabric nomenclature.*

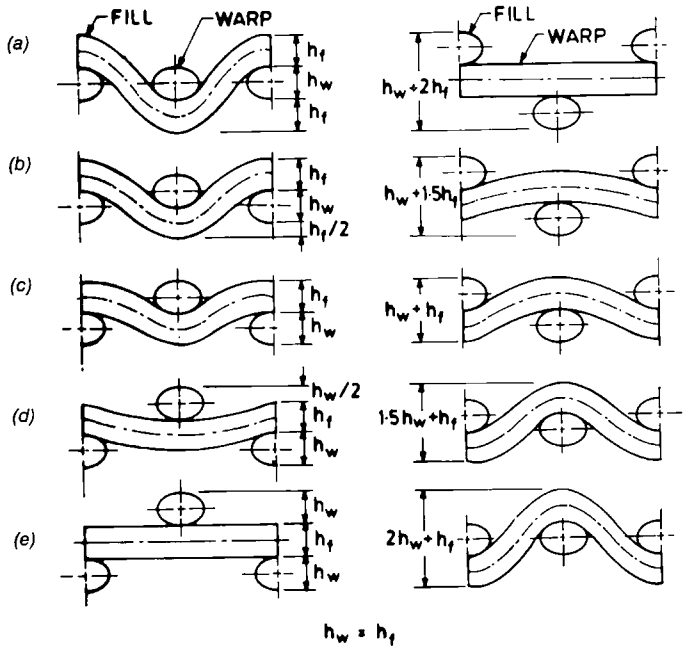

Figure 3. *Effect of crimp on the thickness of woven fabric.*

into account the actual weave geometry including the presence of gap and yarn cross-sectional area. The proposed 2D woven fabric composite models are abbreviated as 2D WF models for further discussion.

Lamina Configuration

In the present work, the discussion is restricted to non-hybrid 2D plain weave fabric lamina, i.e., the warp and fill fiber materials are assumed to be the same. A unit cell of plain weave fabric lamina is shown in Figure 4. The sections at the boundaries of the unit cell are also shown. It can be seen that by inverting section D-C, section A-B can be obtained. Similarly by inverting section A-D, section B-C can be obtained. In order to simplify the analysis, the sections of the unit cell are divided into different regions such as straight cross-ply or UD region, undulated cross-ply or UD region and pure matrix region. The presence of a particular region is dependent on the position of the section in the unit cell. The sections parallel to A-D are divided into different zones marked by a_1 to a_5, the values of which are dependent on the width of the warp yarn (a_w), gap between

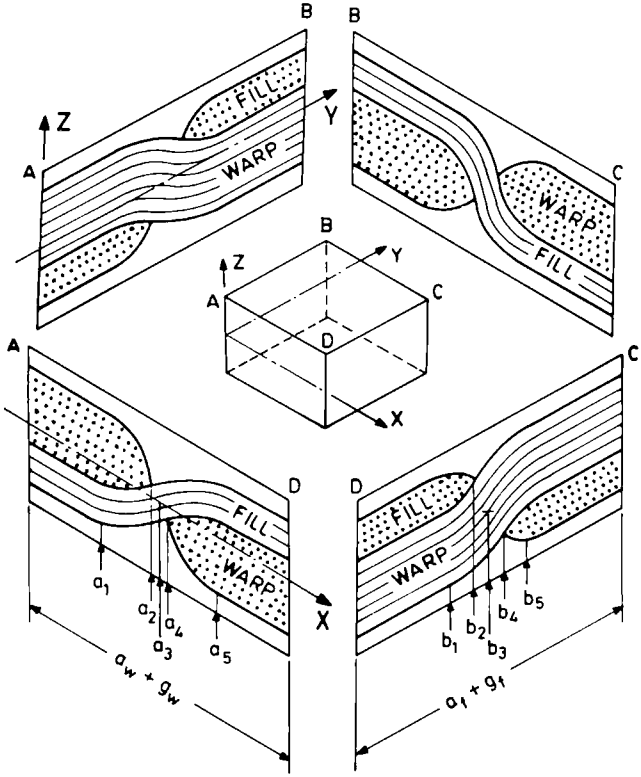

Figure 4. *Unit cell of plain weave fabric lamina.*

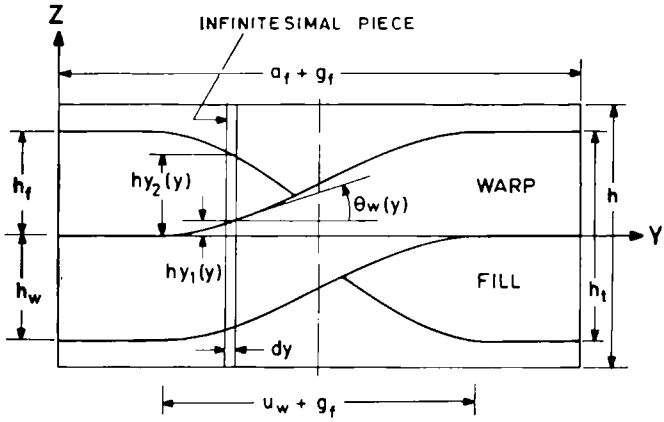

Figure 5. *Section D-C of the unit cell along warp.*

two adjacent warp yarns (g_w) and undulation of fill yarn (u_f). Similarly, the sections parallel to D-C are divided into different zones marked by b_1 to b_5, the values of which are dependent on the width of the fill yarn (a_f), gap between two adjacent fill yarns (g_f) and undulation of warp yarn (u_w). Here, the term "undulation" is used for the undulated length of yarn. The expressions for a_1 to a_5 and b_1 to b_5 are as follows:

$$a_1 = \frac{a_w - u_f}{2} \qquad b_1 = \frac{a_f - u_w}{2}$$

$$a_2 = \frac{a_w}{2} \qquad b_2 = \frac{a_f}{2}$$

$$a_3 = \frac{a_w + g_w}{2} \qquad b_3 = \frac{a_f + g_f}{2} \tag{1}$$

$$a_4 = \frac{a_w}{2} + g_w \qquad b_4 = \frac{a_f}{2} + g_f$$

$$a_5 = \frac{a_w + u_f}{2} + g_w \qquad b_5 = \frac{a_f + u_w}{2} + g_f$$

The configuration of yarns in section D-C (Figure 5) is given by shape functions

similar to those given by Chou and Ishikawa [6]. The undulation of the yarn is of sinusoidal form.

$$hy_1(y) = \begin{cases} h_t/2 - h_f & \ldots\ 0 \le y \le b_1 \\ \left[1 + \sin\left\{(y - b_3)\dfrac{\pi}{u_w + g_f}\right\}\right] h_t/2 + h_t/2 - h_f & \ldots\ b_1 \le y \le b_5 \\ h_t/2 & \ldots\ b_5 \le y \le (a_f + g_f) \end{cases} \tag{2a}$$

$$hy_2(y) = \begin{cases} h_t/2 & \ldots\ 0 \le y \le b_1 \\ [h_t/2 - hy_1(b_2)] \cos\left\{(y - b_1)\dfrac{\pi}{u_w}\right\} + hy_1(b_2) & \ldots\ b_1 \le y \le b_2 \\ -[h_t/2 - hy_1(b_2)] \cos\left\{(y - b_5)\dfrac{\pi}{u_w}\right\} - hy_1(b_2) & \ldots\ b_4 \le y \le b_5 \\ -h_t/2 & \ldots\ b_5 \le y \le (a_f + g_f) \end{cases} \tag{2b}$$

The local angle between the warp yarn and the global coordinate system is given by

$$\theta_w(y) = \tan^{-1}\left(\frac{dhy_1(y)}{dy}\right)$$

$$= \tan^{-1}\left(h_f/2\left(\frac{\pi}{u_w + g_f}\right)\cos\left\{(y - b_3)\frac{\pi}{u_w + g_f}\right\}\right) \tag{3}$$

The configuration of sections across the Y-axis in the region where $a_3 \le x \le (a_w + g_w)$ can be obtained from the configuration of section D-C as given by

Equations (2). The configuration of sections across the Y-axis in the region where $0 \leq x \leq a_3$ can be obtained from the configuration of section A-B.

For $0 \leq y \leq b_3$, the configuration of sections across the Y-axis as shown in Figures 6 and 7(a–c) can be given as

$$hx_1(x,y) = \begin{cases} -\left[1-\sin\left\{(x-a_3)\dfrac{\pi}{u_f+g_w}\right\}\right]\left(\dfrac{hy_2(y)+hy_1(y)}{2}\right)+hy_1(y) & \\ \qquad\qquad \ldots \quad a_3 \leq x \leq a_5 & \\ hy_1(y) \qquad\qquad \ldots \quad a_5 \leq x \leq (a_w+g_w) & \end{cases} \tag{4a}$$

$$hx_2(x,y) = \begin{cases} -[h_w - hy_1(y) + hx_1(a_4,y)]\cos\left\{(x-a_5)\dfrac{\pi}{u_f}\right\} + hx_1(a_4,y) & \\ \qquad\qquad \ldots \quad a_4 \leq x \leq a_5 & \\ hy_1(y) - h_w \qquad\qquad \ldots \quad a_5 \leq x \leq (a_w+g_w) & \end{cases} \tag{4b}$$

The fill yarn thickness in a section is given by

$$h_f(y) = hy_2(y) - hy_1(y) \tag{5}$$

It may be noted that at $y = 0$, the fill yarn thickness is maximum, i.e., $h_f(y =$

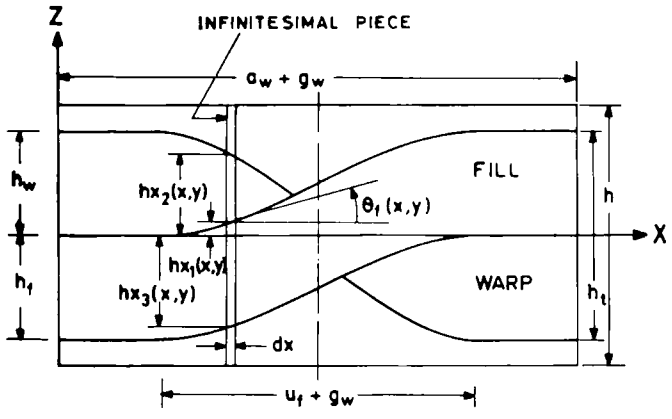

Figure 6. *Section A-D of the unit cell along fill.*

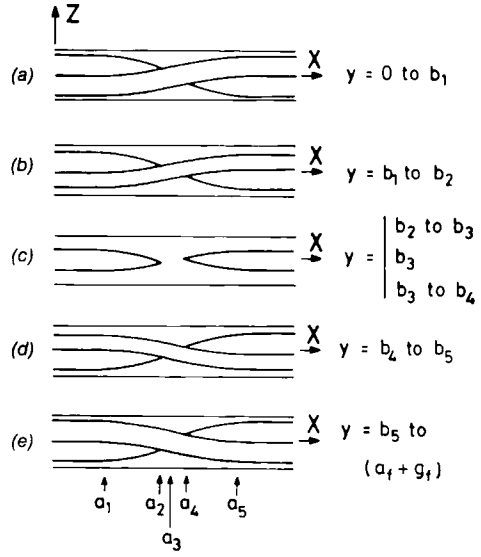

Figure 7. *Sections of the unit cell across Y-axis.*

0) = h_f. The configuration of the fill yarn is defined by $hx_1(x, y)$ and $h_f(y)$. Another function $hx_3(x, y)$ is defined for simplicity as

$$hx_3(x, y) = hx_1(x, y) + h_f(y) \tag{6}$$

Thus, the configuration of yarns in a section is given by $hx_1(x, y)$, $hx_2(x, y)$ and $hx_3(x, y)$. The local angle between the fill yarn and global coordinate system is given by

$$\theta_f(x, y) = \tan^{-1}\left(\frac{dhx_1(x, y)}{dx}\right)$$

$$= \tan^{-1}\left[\frac{hy_2(y) + hy_1(y)}{2} \frac{\pi}{u_f + g_w} \cdot \cos\left\{(x - a_3)\frac{\pi}{u_f + g_w}\right\}\right] \tag{7}$$

Similarly, for $b_3 \le y \le (a_f + g_f)$, the configuration of sections across the *Y*-axis as shown in Figures 7(c–e) can be given by

$$hx_1(x, y) = \begin{cases} -\left[1 - \sin\left\{(x - a_3)\frac{\pi}{u_f + g_w}\right\}\right] \cdot \frac{[hy_1(y) - h_w + hy_2(y)]}{2} \\ \qquad + hy_1(y) - h_w \qquad \ldots \quad a_3 \le x \le a_5 \\ hy_1(y) - h_w \qquad \ldots \quad a_5 \le x \le (a_w + g_w) \end{cases} \tag{8a}$$

$$hx_2(x,y) = \begin{cases} [hy_1(y) - hx_1(a_4,y)] \cos\left\{(x - a_5)\dfrac{\pi}{u_f}\right\} + hx_1(a_4,y) & \ldots \; a_4 \le x \le a_5 \\ hy_1(y) & \ldots \; a_5 \le x \le (a_w + g_w) \end{cases} \tag{8b}$$

The fill yarn thickness in a section is given by

$$h_f(y) = hy_1(y) - hy_2(y) - h_w \tag{9}$$

It can be noted that at $y = a_f + g_f$, the fill yarn thickness is maximum i.e., $h_f(y = a_f + g_f) = h_f$. Here,

$$hx_3(x,y) = hx_1(x,y) - h_f(y) \tag{10}$$

The local angle between the fill yarn and global coordinate system is given by

$$\theta_f(x,y) = \tan^{-1}\left[\frac{hy_2(y) - h_w + hy_1(y)}{2}\frac{\pi}{u_f + g_w} \cdot \cos\left\{(x - a_3)\frac{\pi}{u_f + g_w}\right\}\right] \tag{11}$$

It can be noted that section (c) in Figure 7 can be obtained using Equations (4) and (6) for $b_2 \le y \le b_3$ or using Equations (8) and (10) for $b_3 \le y \le b_4$. For open weaves, $hx_2(x,y)$ gives a steeper contour than $hx_1(x,y)$ due to the shape functions considered. Section (c) in Figure 7 is obtained by using Equations (4) and (6) at $y = b_3$.

2D Woven Fabric (2D WF) Models

In the present analysis, it is assumed that the Classical Lamination Theory (CLT) is applicable to each infinitesimal piece of such sections as shown in Figure 5. The constitutive equations are given by [12]

$$\begin{Bmatrix} N_i \\ M_i \end{Bmatrix} = \begin{bmatrix} A_{ij}(x,y) & B_{ij}(x,y) \\ B_{ij}(x,y) & D_{ij}(x,y) \end{bmatrix} \begin{Bmatrix} \epsilon_j^o \\ k_j \end{Bmatrix} \tag{12}$$

where N_i, M_i are membrane stress and moment resultants. ϵ_j^o, k_j indicate strain and curvature of laminate geometrical mid-plane. The in-plane stiffness constants of the infinitesimal pieces are given by

$$A_{ij}(x,y), B_{ij}(x,y), D_{ij}(x,y) = \int_{-h/2}^{h/2} (1, z, z^2) Q_{ij} dz \tag{13}$$

where $i = 1,2,6$ and $j = 1,2,6$ and

$$Q_{ij} = \begin{bmatrix} E_x/D_\nu & \nu_{yx}E_x/D_\nu & 0 \\ \nu_{yx}E_x/D_\nu & E_y/D_\nu & 0 \\ 0 & 0 & G_{xy} \end{bmatrix} \tag{14}$$

here, $D_\nu = 1 - \nu_{yx}\nu_{xy}$ and $i,j = 1,2,6$.

Q_{ij} of the fill, warp and pure matrix layers of a WF lamina are evaluated based on the corresponding elastic properties and local angle of the yarn. Thus the in-plane stiffness constants in the region where $0 \le y \le b_3$ and $0 \le x \le a_3$ are expressed as

$$\begin{aligned} A_{ij}(x,y) &= \int_{-h/2}^{hx_3(x,y)} Q_{ij}^M dz + \int_{hx_3(x,y)}^{hx_1(x,y)} Q_{ij}^F(x,y)\,dz \\ &\quad + \int_{hx_1(x,y)}^{hx_2(x,y)} Q_{ij}^W(x,y)\,dz + \int_{hx_2(x,y)}^{h/2} Q_{ij}^M dz \\ &= Q_{ij}^M[hx_3(x,y) + h - hx_2(x,y)] \\ &\quad + Q_{ij}^W(x,y)[hx_2(x,y) - hx_1(x,y)] \\ &\quad + Q_{ij}^F(x,y)[hx_1(x,y) - hx_3(x,y)] \end{aligned} \tag{15a}$$

$$\begin{aligned} B_{ij}(x,y) &= \frac{1}{2} Q_{ij}^M[hx_3(x,y)^2 - hx_2(x,y)^2] \\ &\quad + \frac{1}{2} Q_{ij}^W(x,y)[hx_2(x,y)^2 - hx_1(x,y)^2] \\ &\quad + \frac{1}{2} Q_{ij}^F(x,y)[hx_1(x,y)^2 - hx_3(x,y)^2] \end{aligned} \tag{15b}$$

$$\begin{aligned} D_{ij}(x,y) &= \frac{1}{3} Q_{ij}^M \left(hx_3(x,y)^3 - \frac{h^3}{8} - hx_2(x,y)^3\right) \\ &\quad + \frac{1}{3} Q_{ij}^W(x,y)[hx_2(x,y)^3 - hx_1(x,y)^3] \\ &\quad + \frac{1}{3} Q_{ij}^F(x,y)[hx_1(x,y)^3 - hx_3(x,y)^3] \end{aligned} \tag{15c}$$

In a similar way, the expressions for in-plane stiffness constants for the other regions can be written. The second region is $0 \le y \le b_3$ and $a_3 \le x \le (a_w + g_w)$, the third region is $b_3 \le y \le (a_f + g_f)$ and $0 \le x \le a_3$ and the fourth region is $b_3 \le y \le (a_f + g_f)$ and $a_3 \le x \le (a_w + g_w)$.

The effective elastic constants of the fill yarn in the X-direction are given by [13]

$$E_x^F = 1 \Bigg/ \left\{ \frac{\cos \theta_f(x,y)^4}{E_1} + \frac{\sin \theta_f(x,y)^4}{E_3} + \{\cos \theta_f(x,y)^2 \cdot \sin \theta_f(x,y)^2\} \left(\frac{1}{G_{13}} - \frac{2\nu_{31}}{E_3} \right) \right\}$$

$$E_y^F = E_2 \tag{16}$$

$$\nu_{yx}^F = \nu_{21} \cos \theta_f(x,y)^2 + \nu_{32} \sin \theta_f(x,y)^2$$

$$G_{xy}^F = 1 \Bigg/ \left\{ \frac{\sin \theta_f(x,y)^2}{G_{23}} + \frac{\cos \theta_f(x,y)^2}{G_{12}} \right\}$$

Also, the effective elastic constants of the warp in the Y-direction are given by

$$E_y^W = 1 \Bigg/ \left\{ \frac{\cos \theta_w(y)^4}{E_1} + \frac{\sin \theta_w(y)^4}{E_3} + \{\cos \theta_w(y)^2 \cdot \sin \theta_w(y)^2\} \left(\frac{1}{G_{13}} - \frac{2\nu_{31}}{E_3} \right) \right\}$$

$$E_x^W = E_2 \tag{17}$$

$$\nu_{yx}^W = [\nu_{21} \cos \theta_w(y)^2 + \nu_{32} \sin \theta_w(y)^2] \cdot \frac{E_y^W}{E_x^W}$$

$$G_{xy}^W = 1 \Bigg/ \left\{ \frac{\sin \theta_w(y)^2}{G_{23}} + \frac{\cos \theta_w(y)^2}{G_{12}} \right\}$$

The elastic constants in the principal material directions of a UD lamina of the warp or fill yarn can be obtained by using a Composite Cylinder Assemblage (CCA) model using fiber and matrix properties [14,15]. A brief account of the CCA model is given in the Appendix.

The WF lamina is subjected to uniform in-plane loading along the X-axis. The infinitesimal pieces of a section parallel to A-D (Figures 4, 6 and 7) are in series with respect to the loading direction and are assumed to be under constant stress. On the other hand, the infinitesimal pieces of a section parallel to D-C (Figures 4 and 5) are in parallel with respect to the loading direction and the mid-plane

strains of such pieces are assumed to be the same. The assembly of infinitesimal pieces of a section along the loading direction with an iso-stress condition is termed a series model whereas the assembly of infinitesimal pieces of a section across the loading direction with an iso-strain condition is termed a parallel model. In the present work, the following two assembly schemes are used.

In the first scheme, all the infinitesimal pieces of a section along the loading direction are assembled with an iso-stress condition. Then all the sections along the loading direction are assembled with an iso-strain condition. Such a scheme is called a Series-Parallel (SP) model. In the second scheme, all the infinitesimal pieces of a section across the loading direction are assembled with an iso-strain condition. Then all the sections across the loading direction are assembled with an iso-stress condition. Such a scheme is called a Parallel-Series (PS) model. These 2D WF models are described here.

SERIES-PARALLEL (SP) MODEL

The average in-plane compliance constants under a uniformly applied in-plane stress resultant for the sections along the loading direction (Figures 6 and 7) can be obtained as

$$\bar{a}^s_{ij}(y),\ \bar{b}^s_{ij}(y),\ \bar{d}^s_{ij}(y) = \frac{1}{a_w + g_w}\int_0^{a_w+g_w} a_{ij}(x,y),\ b_{ij}(x,y),\ d_{ij}(x,y)\,dx \tag{18}$$

For a plain weave, $\bar{b}^s_{ij}(y)$ becomes zero although locally $b_{ij}(x,y)$ exists. Equation (18) gives the upper bounds of compliance constants for each section. By inverting the average in-plane compliance constants, the lower bounds of in-plane stiffness constants $\bar{A}^s_{ij}(y)$, $\bar{B}^s_{ij}(y)$ and $\bar{D}^s_{ij}(y)$ of the corresponding sections are obtained. The average in-plane stiffness constants of the unit cell/WF lamina are then found by integrating the in-plane stiffness constants of all sections along the Y-axis with an iso-strain condition as follows:

$$\bar{A}^{sp}_{ij},\ \bar{B}^{sp}_{ij},\ \bar{D}^{sp}_{ij} = \frac{1}{a_f + g_f}\int_0^{a_f+g_f} \bar{A}^s_{ij}(y),\ \bar{B}^s_{ij}(y),\ \bar{D}^s_{ij}(y)\,dy \tag{19}$$

where, $\bar{A}^{sp}_{ij}$, $\bar{B}^{sp}_{ij}$ and $\bar{D}^{sp}_{ij}$ are the average in-plane stiffness constants obtained by series-parallel model which gives the lower bounds of in-plane stiffness constants. For a plain weave, $\bar{B}^{sp}_{ij}$ is zero. Inverting the elastic stiffness constants, the upper bounds of in-plane compliance constants can be obtained. The elastic moduli can be obtained from the compliance constants as follows [12]:

$$\begin{aligned} E_x &= 1/(\bar{a}_{11}h) \\ G_{xy} &= 1/(\bar{a}_{66}h) \\ \nu_{xy} &= -\bar{a}_{12}/\bar{a}_{11} \end{aligned} \tag{20}$$

PARALLEL-SERIES (PS) MODEL

The average in-plane elastic stiffness constants of sections parallel to A-B (Figure 4) under the assumption of constant mid-plane strains can be given as

$$\bar{A}^{p}_{ij}(x),\ \bar{B}^{p}_{ij}(x),\ \bar{D}^{p}_{ij}(x) = \frac{1}{a_f + g_f}\int_0^{a_f+g_f} A_{ij}(x,y),\ B_{ij}(x,y),\ D_{ij}(x,y)dy \qquad (21)$$

$\bar{A}^{p}_{ij}(x)$, $\bar{B}^{p}_{ij}(x)$ and $\bar{D}^{p}_{ij}(x)$ give the upper bounds of in-plane stiffness constants of the section at x. For a plain weave, $\bar{B}^{p}_{ij}(x)$ becomes zero. Compliance constants of the sections across the X-axis are obtained by inverting the in-plane stiffness constants. The in-plane compliance constants of the unit cell/WF lamina can be obtained by integrating the compliance constants of all sections across the X-axis under an iso-stress condition as follows:

$$\bar{a}^{ps}_{ij},\ \bar{b}^{ps}_{ij},\ \bar{d}^{ps}_{ij} = \frac{1}{a_w + g_w}\int_0^{a_w+g_w} \bar{a}^{p}_{ij}(x),\ \bar{b}^{p}_{ij}(x),\ \bar{d}^{p}_{ij}(x)dx \qquad (22)$$

where, $\bar{a}^{ps}_{ij}$, $\bar{b}^{ps}_{ij}$ and $\bar{d}^{ps}_{ij}$ are the average in-plane compliance constants of the WF lamina obtained by the parallel-series model which gives the lower bounds of compliance constants. Inverting the compliance constants, the upper bounds of in-plane stiffness constants can be obtained. The elastic constants can be found from compliance constants using Equation (20). It should be noted that the upper and lower bounds given by 2D WF models pertain to the models only.

1D Woven Fabric (1D WF) Models

In 2D WF models, parallel and series models are applied section by section for the unit cell of a WF lamina. In a 1D WF series model, the section having maximum fill yarn thickness [Figure 7(a)] is analyzed using iso-stress conditions. For a WF lamina having balanced close weave fabric, a 1D WF series model and a crimp model (fiber undulation model) given by Ishikawa and Chou [6] become identical. In a 1D WF parallel model, the section having maximum warp yarn thickness (Figure 5) is analyzed using an iso-strain condition.

For a WF lamina having close weave fabric, the 1D WF models tend to a mosaic model [6] when yarn undulation is zero. The mosaic model (parallel and series), 1D WF models (parallel and series) and 2D WF models (series-parallel and parallel-series) give bounds of elastic constants for a WF lamina pertaining to those models. The mosaic models are highly idealized. In the 1D WF models, change in the configuration normal to the section is not considered. The 2D WF models take the actual woven fabric geometry into consideration. Therefore, it is expected that the experimental results would be around 2D WF model predictions.

Overall/Yarn Fiber Volume Fraction

In a WF lamina, the fiber volume fraction varies from section to section as well as within a section. The overall fiber volume fraction (V_f^o) of a WF lamina is the ratio of volume of fibers (warp and fill) to the total volume of the WF lamina. The overall fiber volume fraction can be easily determined experimentally. As the WF lamina consists of cross-ply, UD and pure matrix regions, the fiber volume fraction varies within the lamina. In the elastic analysis of a WF lamina by CLT type models, the elastic properties of UD laminae consisting of warp and fill fibers has to be known. The fiber volume fraction in such a UD lamina here is referred to as yarn fiber volume fraction (V_f^y). The yarn fiber volume fraction is the ratio of volume of fibers (warp/fill) to volume of yarn (warp/fill) including the part of matrix within the yarn. The volume of yarn (warp/fill) can be found from the shape functions by numerical integration. Thus knowing the overall fiber volume fraction (V_f^o) and volume of yarns, the yarn fiber volume fraction (V_f^y) can be obtained. For a constant V_f^o, the yarn fiber volume fraction (V_f^y) depends on the fabric geometry. The effect of weave geometry on V_f^y is discussed in the later section.

The geometry and elastic analysis presented so far are for the unit cell shown in Figure 4. The elastic analysis can be confined to a quarter cell for plain weave fabric lamina with the assumption that the coupling compliance terms are zero over the length of the unit cell. Such an assumption is valid for plain weave fabrics because of symmetry. The unit cell (Figure 4) considered is necessary for the WF laminate analysis which is presented in Part II [16].

Case Studies

The effect of the undulation of the yarn (u_w, u_f) and the lamina thickness on the elastic constants obtained by 1D WF, 2D WF and mosaic models was studied for T-300 carbon/epoxy WF lamina. The fabric was assumed to be a closely woven balanced plain weave. An overall fiber volume fraction of 0.47 was assumed. The following geometry was considered for the plain weave fabric.

$$a = a_w = a_f = 1.0 \text{ mm} \qquad g = g_w = g_f = 0$$

$$V_f^o = 0.47 \qquad n = n_g^W = n_g^F = 2$$

The elastic properties of T-300 carbon fiber and epoxy resin are given in Table 1 [17]. The undulation (u_w, u_f) was varied from 0.1 to a_w (a_f). For this case, $h_w = h_f = 0.05$ mm and $h = 0.1$ mm were considered.

In the second case, the lamina thickness (h) was varied from 0.1 to 0.5 mm where $h_w = h_f = h/2$. The undulation (u_w, u_f) was 0.6 mm for all the lamina thicknesses considered. The yarn fiber volume fraction (V_f^y) was found from V_f^o and fabric geometry. The UD lamina properties corresponding to fiber volume fraction of V_f^y were found using the Composite Cylinder Assemblage (CCA) model. The predicted elastic constants by 1D WF and 2D WF models for different undulations are given in Tables 2 and 3 respectively. Elastic moduli as

Table 1. Elastic properties of fibers and matrix.

Material	E_L GPa	E_T GPa	G_{LT} GPa	G_{TT} GPa	ν_{LT}
T-300 carbon	230.0	40.0	24.0	14.3	0.26
E-glass*	72.0	72.0	27.7	27.7	0.30
Epoxy resin*	3.5	3.5	1.3	1.3	0.35

*Isotropic.

Table 2. Effect of undulation on elastic constants predicted by 1D WF models. (T-300 carbon/epoxy WF lamina, balanced plain weave, $V_f^o = 0.47$, $h/a = 0.1$, $g/a = 0$, $n_g = 2$.)

			Parallel Model			Series Model		
No.	u/a	V_f^y	E_x, E_y GPa	G_{xy} GPa	ν_{xy}	E_x, E_y GPa	G_{xy} GPa	ν_{xy}
1.*	0.00	0.47	60.0	3.16	0.045	27.2	3.13	0.045
2.	0.10	0.49	60.2	3.25	0.047	24.5	3.21	0.064
3.	0.20	0.51	60.4	3.35	0.048	26.2	3.30	0.059
4.	0.25	0.52	60.5	3.41	0.047	27.4	3.35	0.058
5.	0.50	0.57	61.2	3.77	0.047	34.1	3.69	0.059
6.	0.60	0.60	61.6	3.97	0.046	37.2	3.87	0.062
7.	0.80	0.66	62.5	4.52	0.045	44.5	4.39	0.068
8.	1.00	0.74	63.9	5.43	0.045	54.0	5.26	0.077

*Mosaic model.

Table 3. Effect of undulation on elastic constants predicted by 2D WF models. (T-300 carbon/epoxy WF lamina, balanced plain weave, $V_f^o = 0.47$, $h/a = 0.1$, $g/a = 0$, $n_g = 2$.)

			Parallel-Series (PS)			Series-Parallel (SP)		
No.	u/a	V_f^y	E_x, E_y GPa	G_{xy} GPa	ν_{xy}	E_x, E_y GPa	G_{xy} GPa	ν_{xy}
1.*	0.00	0.47	60.0	3.16	0.046	27.2	3.13	0.045
2.	0.10	0.49	42.6	3.18	0.072	23.8	3.19	0.067
3.	0.20	0.51	44.3	3.24	0.066	24.7	3.24	0.063
4.	0.25	0.52	45.8	3.27	0.065	25.4	3.27	0.061
5.	0.50	0.57	51.3	3.46	0.067	28.7	3.45	0.058
6.	0.60	0.60	52.8	3.56	0.068	30.0	3.56	0.058
7.	0.80	0.66	55.1	4.85	0.072	32.7	3.84	0.058
8.	1.00	0.74	57.2	4.34	0.076	35.7	4.34	0.061

*Mosaic model.

Table 4. Effect of lamina thickness on elastic constants predicted by 1D WF models. (T-300 carbon/epoxy WF lamina, balanced plain weave, $V_f^\circ = 0.47$, $V_f^y = 0.6$, $u/a = 0.6$, $g/a = 0$, $n_g = 2$.)

		Parallel Model			Series Model		
No.	*h/a*	E_x, E_y GPa	G_{xy} GPa	ν_{xy}	E_x, E_y GPa	G_{xy} GPa	ν_{xy}
1.	0.1	61.5	3.97	0.046	37.2	3.87	0.062
2.	0.2	61.5	3.97	0.052	31.1	3.87	0.067
3.	0.3	61.5	3.97	0.057	26.2	3.87	0.074
4.	0.4	61.5	3.97	0.060	22.6	3.87	0.081
5.	0.5	61.5	3.97	0.064	20.3	3.87	0.088

a function of lamina thickness are given in Tables 4 and 5. The corresponding V_f^y are also given in these tables. The elastic constants predicted using mosaic model are given in Table 6.

EXPERIMENTAL WORK

Experiments were carried out to study the validity of analytical models. In this work plain weave fabrics of E-glass and T-300 carbon were used. Three types of E-glass woven fabrics and one type of T-300 carbon woven fabric were considered. The yarn and the fabric geometries are given in Table 7. The resin used was LY-556 with hardener HY-951 supplied by Cibatul, India. WF laminae and laminates of E-glass/epoxy and carbon/epoxy were made by compression molding. Curing of the WF laminae and laminates was done at room temperature (27°C). The WF lamina properties are given in Table 8.

Tensile test specimens were cut from WF laminae and laminates along both the warp and fill directions as per ASTM Test D 3039. The thicknesses of the WF laminae were less than the minimum required as per ASTM Test D 3039, but for comparison purpose, the same standard was used for WF laminae also. Strain

Table 5. Effect of lamina thickness on elastic constants predicted by 2D WF models. (T-300 carbon/epoxy WF lamina, balanced plain weave, $V_f^\circ = 0.47$, $V_f^y = 0.6$, $u/a = 0.6$, $g/a = 0$, $n_g = 2$.)

		Parallel-Series (PS)			Series-Parallel (SP)		
No.	*h/a*	E_x, E_y GPa	G_{xy} GPa	ν_{xy}	E_x, E_y GPa	G_{xy} GPa	ν_{xy}
1.	0.1	52.8	3.56	0.068	30.0	3.56	0.058
2.	0.2	39.9	3.56	0.076	25.4	3.56	0.072
3.	0.3	30.8	3.56	0.090	21.7	3.56	0.086
4.	0.4	25.2	3.56	0.089	19.0	3.56	0.099
5.	0.5	21.9	3.56	0.093	17.3	3.56	0.110

Table 6. Elastic constants predicted by mosaic models. (T-300 carbon/epoxy WF lamina, balanced plain weave, $V_f^o = V_f^y$, $g/a = 0$, $n_g = 2$.)

No.	V_f^o	Parallel Model E_x, E_y GPa	Parallel Model G_{xy} GPa	Parallel Model ν_{xy}	Series Model E_x, E_y GPa	Series Model G_{xy} GPa	Series Model ν_{xy}
1.	0.47	60.0	3.16	0.045	27.2	3.13	0.045
2.	0.49	62.3	3.29	0.045	28.2	3.25	0.045
3.	0.51	64.6	3.43	0.045	29.3	3.40	0.045
4.	0.52	65.9	3.51	0.045	29.9	3.48	0.045
5.	0.57	73.0	4.02	0.045	33.4	3.98	0.045
6.	0.60	76.5	4.30	0.045	35.2	4.26	0.045
7.	0.66	84.0	5.02	0.046	39.3	4.98	0.046
8.	0.74	94.3	6.34	0.048	45.4	6.28	0.048

Table 7. Yarn and fabric geometries. (Plain weave fabric, $h_w = h_f = h_t/2$.)

Fabric Material	Fabric Thickness (h_t), mm	Counts/cm Warp	Counts/cm Fill	Width of Yarn, mm Warp (a_w)	Width of Yarn, mm Fill (a_f)	Gap, mm Warp (g_w)	Gap, mm Fill (g_f)	Fabric Weight g/m²
1) T-300 carbon	0.15	9.00	9.00	1.10	0.96	0.011	0.151	120
2) E-glass								
a)	0.18	17.00	13.00	0.59	0.52	0.0	0.25	205
b)	0.50	6.40	5.80	1.44	1.12	0.12	0.60	470
c)	0.10	13.75	13.75	0.50	0.50	0.23	0.23	94

Table 8. Properties of WF lamina.

Material System	Fabric Thickness (h_t), mm	Lamina Thickness (h), mm	Overall Fiber Volume Fraction (V_f^o)
1) T-300 carbon/epoxy	0.15	0.16	0.44
2) E-glass/epoxy			
a)	0.18	0.20	0.38
b)	0.50	0.50	0.39
c)	0.10	0.15	0.25

gages were mounted along longitudinal and lateral directions. Static tension tests were performed on a JJ Lloyed M 50 K machine. The specimens were tested at room temperature (27°C) at a cross head speed of 1 mm/min. A total of 100 specimens was prepared and tested. Stress-strain behavior was recorded. Elastic constants along the warp and fill directions were found.

The fiber volume fraction for T-300 carbon/epoxy and E-glass/epoxy were obtained by using acid digestion and burn off techniques respectively.

Optical photomicrographs of cross sections of WF laminates were obtained to study the yarn configuration. Figure 8 shows a typical photomicrograph of T-300 carbon/epoxy plain weave fabric laminate.

RESULTS AND DISCUSSION

The photomicrograph of T-300 carbon/epoxy plain weave fabric laminate shows a change in the configuration from one lamina to another (Figure 8). This indicates that the change in configuration both along as well as across the yarns (warp/fill) is significant and the two-dimensional extent of the fabric should be taken into account in the WF lamina analysis.

Using 1D WF, 2D WF, and mosaic models, the elastic constants are predicted for different undulations and lamina thicknesses for T-300 carbon/epoxy WF lamina. The effect of undulation on yarn fiber volume fraction (V_f^y) can be seen from Table 2. For a constant V_f^o, as undulation increases, pure matrix volume increases and thereby V_f^y increases. It can be seen from Tables 2, 3 and 6 that for a constant V_f^y, the predicted elastic moduli follow the following order:

$$\begin{matrix}\text{Mosaic}\\ \text{Parallel}\end{matrix} > \begin{matrix}\text{1D WF}\\ \text{Parallel}\end{matrix} > \begin{matrix}\text{2D WF}\\ \text{PS}\end{matrix} > \begin{matrix}\text{Mosaic}\\ \text{Series}\end{matrix} > \begin{matrix}\text{1D WF}\\ \text{Series}\end{matrix} > \begin{matrix}\text{2D WF}\\ \text{SP}\end{matrix}$$

The reasons for such a trend are discussed below. In the mosaic-parallel model, undulation of yarns is neglected. The local coupling between bending and stretching also does not affect the predicted elastic constants whereas in the 1D WF parallel model, the undulation is taken into account although the local coupling still does not affect the predicted elastic constants. In the 2D WF models, the change in the configuration from section to section is taken into account. In the 2D WF PS model, upper bounds of in-plane stiffness constants of each section are found first. Subsequently, when the series model is applied to such sections, the sections having lower stiffness constants i.e., higher compliance constants, have a significant effect on the in-plane stiffness constants of a WF lamina which tend to reduce them. Thus the mosaic parallel model prediction is higher than the 1D WF parallel model prediction which in turn is higher than the 2D WF PS model prediction.

In the mosaic series model, although the undulation is neglected, the local coupling effect reduces the predicted elastic moduli. In the 1D WF series model, the prediction is still lower since the undulation is taken into account. Finally, the 2D WF SP model gives the lowest elastic constants since the undulation in both the warp and fill directions is considered.

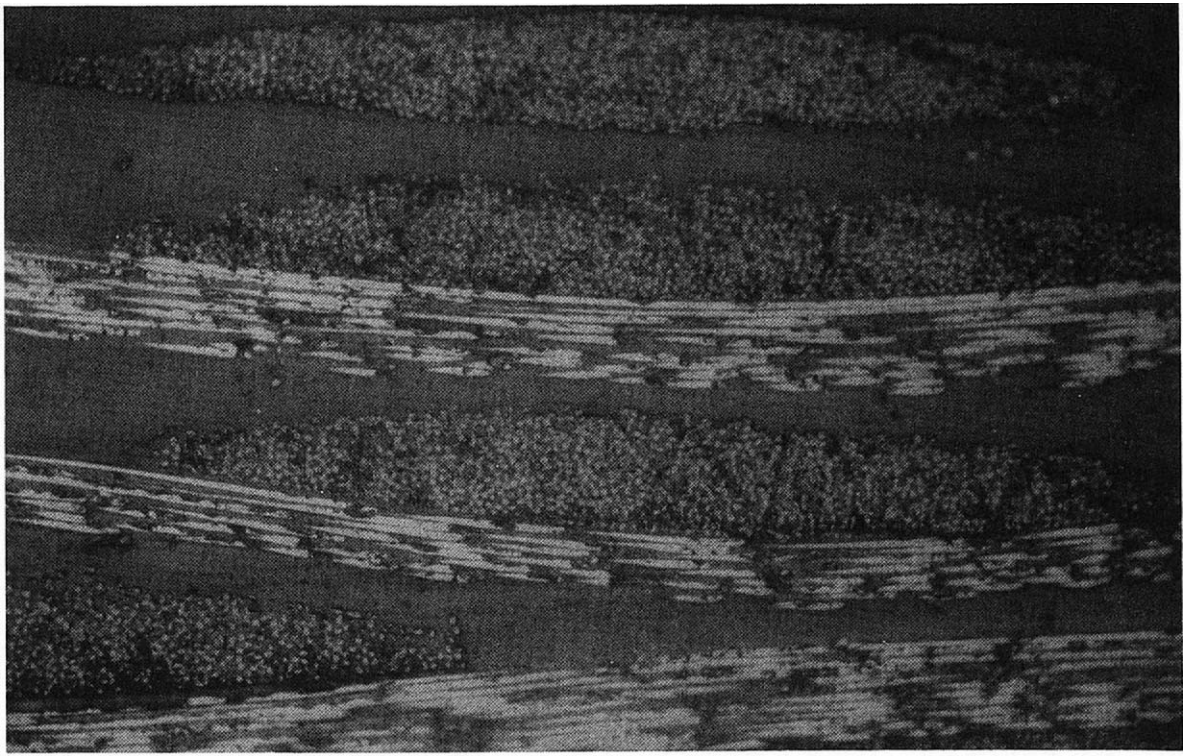

Figure 8. *Photomicrograph of a section of T-300 carbon/epoxy plain weave fabric laminate.*

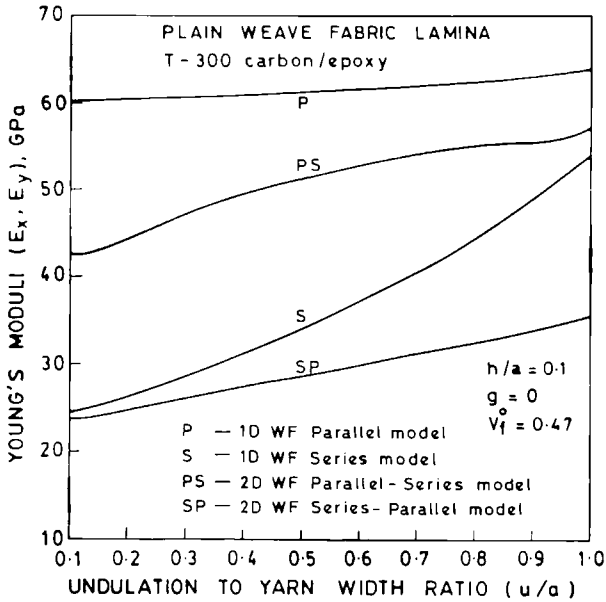

Figure 9. *Effect of undulation on elastic moduli.*

The effect of undulation on the elastic constants predicted by 1D and 2D WF models can be seen in Figure 9 and Tables 2 and 3. As V_f^y increases with increase in undulation for a constant V_f^o, the elastic moduli predicted by the 1D parallel model increase. With increase in yarn undulation the change in local fiber angle is gradual and the magnitude of local fiber angle is reduced. In other words, the yarn tends to become straight. The local coupling effect is also reduced as the yarn undulation increases. The combined effect is the increase in elastic moduli as predicted by the 1D WF series model. The increase in elastic moduli is more in the case of the 1D WF series model than in the 1D WF parallel model. The effect of undulation in the case of 1D WF models is carried to 2D WF models. Thus, with the increase in undulation the elastic moduli predicted by 1D and 2D WF models increase.

When the undulation is zero, 1D and 2D WF models become identical with 1D and 2D mosaic models respectively. For a practically feasible weave, certain minimum undulation is necessary, the amount of which depends on the lamina thickness. Also, the shape functions assumed for the yarns do not apply when the undulation is very small.

The effect of lamina thickness on the elastic moduli predicted by 1D and 2D WF models can be seen from Figure 10 and Tables 4 and 5. With the same V_f^o, the yarn fiber volume fraction (V_f^y) remains constant for all h/a ratios. The elastic moduli predicted by the 1D WF parallel model do not change with lamina thickness since V_f^y remains constant. It may be noted that undulation affects V_f^y and

thereby the elastic moduli predicted by the 1D WF parallel model. With increase in the lamina thickness, the change in the local fiber angle is not gradual and the magnitude of it is also increased. Therefore the elastic moduli predicted by the 1D WF series model reduce with increase in lamina thickness. In the 2D WF PS model, although the parallel model is applied first, the sections having lower stiffness constants appear in series leading to the reduction in the stiffness. Such an effect becomes more predominant as the lamina thickness is increased. In the case of a 2D WF SP model, as the series model is applied first, the elastic moduli of each section are reduced. Such an effect becomes predominant with increase in the lamina thickness. Thus in the case of the series model and 2D WF models, the elastic moduli reduce with increase in the lamina thickness.

The modulus of rigidity follows a similar trend as that of the modulus of elasticity. The modulus of rigidity, as predicted by 1D and 2D WF models, increases with increase in the undulation (Tables 2 and 3). With the increase in undulation, the Poisson's ratio initially increases and then decreases as predicted by the 1D WF parallel model whereas the Poisson's ratio predicted by the 1D WF series model and 2D WF models initially decreases and then increases as undulation is increased. The modulus of rigidity does not depend upon the lamina thickness as predicted by 1D and 2D WF models whereas the Poisson's ratio increases with increase in lamina thickness (Tables 4 and 5).

Tables 9 and 10 give the elastic moduli determined experimentally and predicted by 1D and 2D WF models. The yarns in the cases of material systems 1,

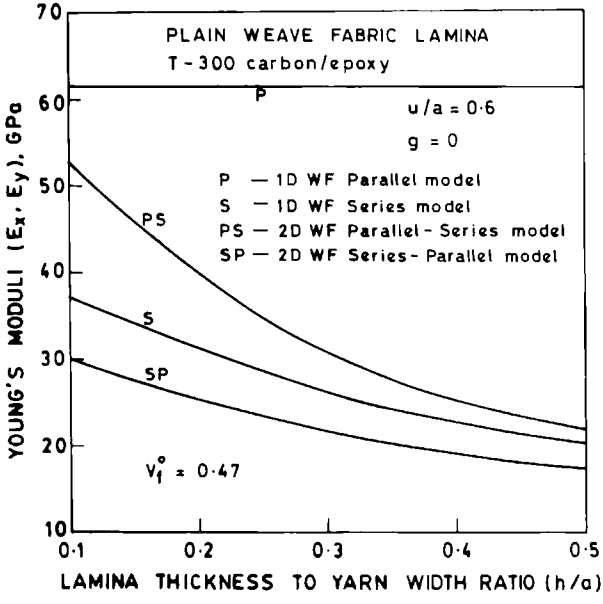

Figure 10. *Effect of lamina thickness on elastic moduli.*

Table 9. Elastic modulus predicted by WF models in comparison with experimental data—E_y, GPa (along warp).

Material System	Lamina Thickness (h), mm	Experimental Average (Range)	Predicted			
			P	S	PS	SP
1) T-300 carbon/epoxy	0.16	60.3 (56–61)	67.8	54.7	58.8	38.2
2) E-glass/epoxy						
a)	0.20	18.1 (15–22)	28.6	24.1	21.5	18.4
b)	0.50	14.8 (14–22)	29.5	24.4	21.6	18.4
c)	0.15	14.5 (10–16)	21.1	23.1	14.9	13.9

2a and 2c were composed of continuous untwisted filaments. The fabric in the case 2b had twisted yarn. An appropriate fiber-to-yarn stiffness efficiency factor should be used to take the effect of yarn structure into account. In the present study, the fiber-to-yarn stiffness efficiency factor of one was used for all the cases including the material system 2b. In other words, it was assumed that the fiber and yarn properties were the same.

It is interesting to note that the material system used and the presence of a gap between two adjacent yarns can have a significant effect on the trend of results. In the case of T-300 carbon/epoxy, as g_w is very small, E_y predicted by 1D and 2D WF models (Table 9) follows the same trend as discussed earlier. On the other hand, as g_f is higher, the trend for E_x is different. In this case the PS model prediction is lower than the 1D WF series model prediction (Table 10).

Table 10. Elastic modulus predicted by WF models in comparison with experimental data—E_x, GPa (along fill).

Material System	Lamina Thickness (h), mm	Experimental Average (Range)	Predicted			
			P	S	PS	SP
1) T-300 carbon/epoxy	0.16	49.3 (47–50)	54.1	51.5	45.8	31.1
2) E-glass/epoxy						
a)	0.20	—	22.1	26.8	17.1	16.7
b)	0.50	13.8 (12–16)	22.1	26.3	16.1	15.7
c)	0.15	14.5 (10–16)	21.1	23.1	14.9	13.9

For E-glass/epoxy, 1D WF models predict higher elastic moduli compared to 2D WF models. The 1D WF parallel model predicts higher elastic moduli. The effect of gap is felt only on straightening of the yarn along the loading direction in the 1D WF series model. In the 1D WF parallel model, the effect of gap on the reduction in fiber volume fraction is felt for that section. Hence the predictions of the 1D WF series model can be higher than the 1D WF parallel model.

A large discrepancy between the predictions of elastic moduli of plain weave fabric lamina using the crimp model and the experimental results was reported by Ishikawa et al. [18]. A similar discrepancy is found between the predicted elastic moduli by 1D WF models and the experimental results (Tables 9 and 10). On the other hand, the correlation between experimental results and elastic moduli predicted by 2D WF models is fairly good. The predictions of PS and SP models are close to each other for WF lamina made of isotropic fibers i.e., E-glass in this case. The predictions of the SP model are lower than those of the PS model for the case of transversely isotropic fibers i.e., T-300 carbon. There is a significant effect of the material system and the extent of gap on the predictions of different models. In general, the PS model is recommended for the prediction of elastic moduli of the WF lamina.

CONCLUSIONS

1. The yarn fiber volume fraction (V_f^y) depends on the weave geometry for a constant overall fiber volume fraction (V_f^o). As the undulation of yarn increases, V_f^y increases for a constant V_f^o. For constant V_f^o and undulation, V_f^y remains constant for all h/a ratios.
2. The elastic moduli predicted by different models follow a trend such that

$$\begin{matrix}\text{Mosaic}\\ \text{Parallel}\end{matrix} > \begin{matrix}\text{1D WF}\\ \text{Parallel}\end{matrix} > \begin{matrix}\text{2D WF}\\ \text{PS}\end{matrix} > \begin{matrix}\text{Mosaic}\\ \text{Series}\end{matrix} > \begin{matrix}\text{1D WF}\\ \text{Series}\end{matrix} > \begin{matrix}\text{2D WF}\\ \text{SP}\end{matrix}$$

3. As the undulation increases, the elastic moduli predicted by 1D and 2D WF models increase.
4. As the lamina thickness increases, the elastic moduli predicted by 1D WF series model and 2D WF models reduce and those predicted by 1D WF parallel model remain constant.
5. PS model is recommended for the prediction of in-plane elastic constants of the WF lamina.

NOMENCLATURE

$A_{ij}(x, y)$ = local in-plane stiffness
$\bar{A}_{ij}$ = averaged in-plane stiffness of a WF lamina
$\bar{A}_{ij}(\ )$ = averaged in-plane stiffness of a section
$a_{ij}(x, y)$ = local in-plane compliance
$\bar{a}_{ij}$ = averaged in-plane compliance of a WF lamina
$\bar{a}_{ij}(\ )$ = averaged in-plane compliance of a section
a = width of a yarn

a_1 to a_5 = different zones along X-axis
$B_{ij}(x, y)$ = local bending/stretching coupling stiffness
$\bar{B}_{ij}$ = averaged bending/stretching coupling stiffness of a WF lamina
$\bar{B}_{ij}(\ )$ = averaged bending/stretching coupling stiffness of a section
$b_{ij}(x, y)$ = local bending/stretching coupling compliance
$\bar{b}_{ij}$ = averaged bending/stretching coupling compliance of a WF lamina
$\bar{b}_{ij}(\ )$ = averaged bending/stretching coupling compliance of a section
b_1 to b_5 = different zones along Y-axis
$D_{ij}(x, y)$ = local bending stiffness
$\bar{D}_{ij}$ = averaged bending stiffness of a WF lamina
$\bar{D}_{ij}(\ )$ = averaged bending stiffness of a section
$d_{ij}(x, y)$ = local bending compliance
$\bar{d}_{ij}$ = averaged bending compliance of a WF lamina
$\bar{d}_{ij}(\ )$ = averaged bending compliance of a section
E = Young's modulus
G = modulus of rigidity
g = gap between two adjacent yarns
$hx_1(x, y), hx_2(x, y), hx_3(x, y)$ = yarn shape functions along X-axis
h = total thickness of a woven fabric lamina
h_f = maximum thickness of the fill yarn
$h_f(y)$ = thickness of the fill yarn for a section at y
h_t = fabric thickness
$hy_1(y), hy_2(y)$ = yarn shape functions along Y-axis
h_w = maximum thickness of the warp yarn
k = transverse bulk modulus
k_j = curvature at the laminate geometrical mid-plane
M_i = moment resultant
N_i = membrane stress resultant
n_g = number of geometrical repeats in fabric structure
Q_{ij} = elastic stiffness matrix
u = undulated length of the yarn
V_f = fiber volume fraction
V_m = matrix volume fraction
x, y, z = Cartesian coordinates
ϵ_j^o = strain components at the laminate geometrical mid-plane
ν = Poisson's ratio
$\theta_f(x, y)$ = local angle between the fill yarn and global coordinate system
$\theta_w(y)$ = local angle between the warp yarn and global coordinate system

Subscripts

f = quantities of the fill yarn
L = quantities in longitudinal direction
m = quantities of matrix
T = quantities in transverse direction
w = quantities of the warp yarn
1, 2, 3 = principal material coordinates

Superscripts

F = quantities of the fill yarn
f = quantities of fiber
M, m = quantities of matrix
o = overall property
p = quantities obtained by 1D WF parallel model
ps = quantities obtained by parallel-series model
sp = quantities obtained by series-parallel model
s = quantities obtained by 1D WF series model
W = quantities of the warp yarn
$\underline{y}$ = yarn property
$\bar{}$ = over bar indicates average quantity

ABBREVIATIONS

CCA—Composite Cylinder Assemblage (- model)
CLT—classical lamination theory
P—(1D WF) parallel (- model)
PS—parallel-series (- model)
S—(1D WF) series (- model)
SP—series-parallel (- model)
UD—unidirectional
WF—woven fabric
1D—one-dimensional
2D—two-dimensional

ACKNOWLEDGEMENTS

The project was supported by the Structures Panel, Aeronautics R&D Board (ARDB), Ministry of Defence, Government of India, Grant No. AERO/RD-134/100/10/90-91/659.

APPENDIX

The Composite Cylinder Assemblage (CCA) model [14,15] gives simple closed form analytical expressions for the effective moduli E_L, G_{LT}, ν_{LT} and k while the moduli G_{TT} and E_T are bracketed by close bounds. Here, the UD lamina is modeled as an assemblage of long composite cylinders consisting of the inner circular fiber and the outer concentric matrix shell. The fiber and matrix are considered to be transversely isotropic.

The transverse bulk modulus of the UD lamina is given by,

$$k = \frac{k^m(k_f + G^m_{TT})(1 - V_f) + k^f(k^m + G^m_{TT})V_f}{(k^f + G^m_{TT})(1 - V_f) + (k^m + G^m_{TT})V_f}$$

here,

$$\frac{1}{k^f} = -\frac{1}{G^f_{TT}} - \frac{4\nu^{f^2}_{LT}}{E^f_L} + \frac{4}{E^f_T}$$

$$\frac{1}{k^m} = -\frac{1}{G^m_{TT}} - \frac{4\nu^{m^2}_{LT}}{E^m_L} + \frac{4}{E^m_T}$$

The longitudinal Young's modulus of the UD lamina is given by,

$$E_L = E^f_L V_f + E^m_L V_m + \frac{4(\nu^f_{LT} - \nu^m_{LT})^2 V_m V_f}{V_m/k^f + V_f/k^m + 1/G^m_{TT}}$$

The longitudinal Poisson's ratio and the modulus of rigidity are given by,

$$\nu_{LT} = \nu^f_{LT} V_f + \nu^m_{LT} V_m + \frac{(\nu^f_{LT} - \nu^m_{LT})(1/k^m - 1/k^f) V_f V_m}{V_m/k^f + V_f/k^m + 1/G^m_{TT}}$$

$$G_{LT} = G^m_{LT} \cdot \frac{G^m_{LT} V_m + G^f_{LT}(1 + V_f)}{G^m_{LT}(1 + V_f) + G^f_{LT} V_m}$$

The transverse shear modulus and the transverse Young's modulus are bracketed by close bounds. The bounds of G_{TT} are given by,

$$G_{TT(-)} = G^m_{TT} + \frac{V_f}{\{1/(G^f_{TT} - G^m_{TT})\} + (k^m + 2G^m_{TT})V_m/\{2G^m_{TT}(k^m + G^m_{TT})\}}$$

$$G_{TT(+)} = G^m_{TT}\left(1 + \frac{(1 + \beta_1)V_f}{\varrho - V_f\{1 + (3\beta_1^2 V_m^2)/(\alpha V_f^3 + 1)\}}\right)$$

when,

$$G^f_{TT} > G^m_{TT} \qquad \text{and} \qquad k^f > k^m$$

whereas,

$$G_{TT(+)} = G^m_{TT} + \frac{V_f}{\{1/(G^f_{TT} - G^m_{TT})\} + (k^m + 2G^m_{TT})V_m/\{2G^m_{TT}(k^m + G^m_{TT})\}}$$

$$G_{TT(-)} = G^m_{TT}\left(1 + \frac{(1 + \beta_1)V_f}{\varrho - V_f\{1 + (3\beta_1^2 V_m^2)/(\alpha V_f^3 - \beta_1)\}}\right)$$

when,

$$G^f_{TT} < G^m_{TT} \qquad \text{and} \qquad k^f < k^m$$

Here,

$$\alpha = \frac{\beta_1 - \gamma\beta_2}{1 + \gamma\beta_2} \qquad \varrho = \frac{\gamma + \beta_1}{\gamma - 1}$$

$$\beta_1 = \frac{k^m}{k^m + 2G^m_{TT}} \qquad \beta_2 = \frac{k^f}{k^f + 2G^f_{TT}}$$

$$\gamma = G^f_{TT}/G^m_{TT} \qquad V_m = 1 - V_f$$

The bounds of E_T are given by

$$E_{T(\pm)} = \frac{4kG_{TT(\pm)}}{k + mG_{TT(\pm)}}$$

where,

$$m = 1 + \frac{4k\nu^2_{LT}}{E_L}$$

Here, the direction L corresponds to the direction 1 and the direction T corresponds to the direction 2 as well as direction 3 in the principal material coordinates.

REFERENCES

1. Raju, I. S., R. L. Foye and V. S. Avva. 1990. "A Review of the Analytical Methods for Fabric and Textile Composites," *Proceedings of the Indo-US Workshop on Composites for Aerospace Application: Part I, Bangalore*, pp. 129–159.
2. Halpin, J. C., K. Jerine and J. M. Whitney. 1971. "The Laminate Analogy for 2 and 3 Dimensional Composite Materials," *J. Composite Mater.*, 5:36.
3. Ishikawa, T. and T. W. Chou. 1983. "One-Dimensional Micromechanical Analysis of Woven Fabric Composites," *AIAA J.*, 21:1714.
4. Ishikawa, T. and T. W. Chou. 1982. "Stiffness and Strength Behaviour of Woven Fabric Composites," *J. Mater. Sci.*, 17:3211.
5. Ishikawa, T. and T. W. Chou. 1982. "Elastic Behaviour of Woven Hybrid Composites," *J. Composite Mater.*, 16:2.
6. Chou, T. W. and T. Ishikawa. 1989. "Analysis and Modeling of Two-Dimensional Fabric Composites," in *Textile Structural Composites*, T. W. Chou and F. K. Ko, eds., Amsterdam: Elsevier Science Publishers, pp. 209–264.
7. Kabelka, J. 1984. "Prediction of the Thermal Properties of Fibre-Resin Composites," in *Developments in Reinforced Plastics–3*, G. Pritchard, ed., London: Elsevier Applied Science Publishers, pp. 167–202.

8. Whitcomb, J. D. 1989. "Three Dimensional Stress Analysis of Plain Weave Composites," paper presented at the *3rd Symposium on Composite Materials: Fatigue and Fracture, Orlando, FL.*
9. Dow, N. F. and V. Ramnath. 1987. "Analysis of Woven Fabrics for Reinforced Composite Materials," NASA-CR-178275.
10. Zhang, Y. C. and J. Harding. 1990. "A Numerical Micromechanics Analysis of the Mechanical Properties of a Plain Weave Composite," *Computers and Structures*, 36:839.
11. Blinov, I. and S. Belay. 1988. ***Design of Woven Fabrics***. Moscow: MIR Publishers.
12. Tsai, S. W. and H. T. Hahn. 1980. *Introduction to Composite Materials*. Lancaster, PA: Technomic Publishing Co., Inc.
13. Lekhnitskii, S. G. 1981. *Theory of Elasticity of an Anisotropic Body*. Moscow: MIR Publishers.
14. Hashin, Z. 1972. "Theory of Fibre Reinforced Materials," CR-1974, NASA.
15. Hashin, Z. 1983. "Analysis of Composite Materials—A Survey," *J. Appl. Mech.*, 50:481.
16. Shembekar, P. S. and N. K. Naik. 1992. "Elastic Behavior of Woven Fabric Composites: II—Laminate Analysis," *J. Composite Mater.*, 26(15):2226–2246.
17. 1989. *Engineered Materials Handbook, Volume 1, Composites*. Ohio: ASM International.
18. Ishikawa, T., M. Matsushima, Y. Hayashi and T. W. Chou. 1985. "Experimental Confirmation of the Theory of Elastic Moduli of Fabric Composites," *J. Composite Mater.*, 19:443.